Spring 2020

Investigation of MnxNi1-xO Thin Films Using Pulsed Laser Deposition

Md Ashif Anwar
Missouri State University, MdAshif14@live.missouristate.edu

INVESTIGATION OF $Mn_xNi_{1-x}O$ THIN FILMS USING PULSED LASER DEPOSITION

A Master's Thesis

Presented to

The Graduate College of

Missouri State University

In Partial Fulfillment

Of the Requirements for the Degree

Master of Science, Materials Science

By

Md Ashif Anwar

May 2020

INVESTIGATION OF $Mn_xNi_{1-x}O$ THIN FILMS USING PULSED LASER DEPOSITION

Physics, Astronomy, and Materials Science

Missouri State University, May 2020

Master of Science

Md Ashif Anwar

ABSTRACT

The exchange bias (EB) effect, especially in nanomaterials, is highly promising for use in antiferromagnet-based spintronics applications. NiO is a well known antiferromagnetic material with a high Néel temperature (525K) and can exhibit ferromagnetism/ ferrimagnetism by adding other magnetic transition elements. Our previous work has shown that the antiferromagnetic characteristics of conventional NiO insulating nanostructured material can be altered to have substantial ferrimagnetic characteristics by doping NiO with Mn or Co. Pulsed laser deposition (PLD) was used to grow heterostructures comprised of a nanostructured thin NiO film deposited on the surface of a MgO (100) and Al_2O_3 (111) substrates, followed by the deposition of a $Mn_xNi_{1-x}O$ thin film layer on top of the NiO layer. X-ray diffraction (XRD), scanning electron microscopy (SEM), and SQUID magnetometry were used to study the structural, morphological, and magnetic properties, respectively, of the thin film heterostructures. XRD and SEM characterizations show that the NiO/$Mn_xNi_{1-x}O$ bilayers were grown quasi-epitaxially on the MgO and Al_2O_3 substrates. The primary motivation of this study is to determine how the magnetic properties and the exchange bias effect may depend upon the interface morphology, structural characteristics and Mn concentration of the $Mn_xNi_{1-x}O$ layer in the heterostructures.

KEYWORDS: Thin films, XRD, SEM, SQUID, Pulsed Laser Deposition

INVESTIGATION OF $Mn_xNi_{1-x}O$ THIN FILMS USING PULSED LASER DEPOSITION

By

Md Ashif Anwar

A Master's Thesis
Submitted to the Graduate College
Of Missouri State University
In Partial Fulfillment of the Requirements
For the Degree of Master of Science, Materials Science

May 2020

Approved:

Robert A. Mayanovic, Ph.D., Thesis Committee Chair

Kartik C. Ghosh, Ph.D., Committee Member

Tiglet Besara, Ph.D., Committee Member

Julie Masterson, Ph.D., Dean of the Graduate College

ACKNOWLEDGEMENTS

I would like to dedicate this thesis to my parents who always supported me throughout my life. I also like to acknowledge and thank PAMS faculty and staff at Missouri State University for providing facilities and opportunities to complete my graduate studies.

TABLE OF CONTENTS

LIST OF TABLES

LIST OF FIGURES

INTRODUCTION

Nanoscale materials are highly useful for a number of important magnetic applications. Thin film heterostructures, on the scale of nanometers, are presently used for high density data storage (HDDS), magnetic random-access memory (MRAM), spin valves, semiconductor spintronics, antiferromagnetic spintronics, magneto-sensors and other devices[1,2,3]. The lattice mismatch causes lattice strain in the thin film heterostructures and lattice strain in the film increases with film thickness. Therefore, lattice strain in very thin film heterostructures is less evident and subsequently relaxed up to a certain critical thickness. Thus, thin film heterostructures in the nanoscale range have enhanced magnetic properties (e.g., coercivity, remanent magnetization, etc.) that are proving to be highly useful for the above-mentioned applications [4].

The exchange bias phenomenon, as first proposed by Meiklejohn and Bean [5], is deemed to have high potential for application in magnetic-based devices. There is no precise theory to account for the effect: however, many models have been proposed to explain the physical origin of exchange bias. The strong coupling (also called the pinning effect) between the antiferromagnetic (AFM) and ferromagnetic (FM) or ferrimagnetic (FiM) spins at the interface is the generally accepted model of the exchange bias effect. Consider the interface between an AFM and FM layer, as shown in Figure 1.1, when the temperature is above the Néel temperature (T_N), which characterizes the AFM to paramagnetic phase transition, and below the Curie temperature (T_C), which characterizes the FM to paramagnetic phase transition.

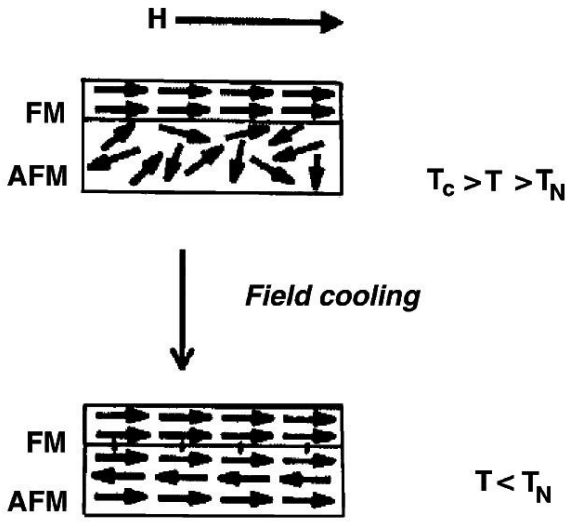

Figure 1.1. The spin configurations of an FM–AFM couple before and after the field cooling [4].

At this temperature, the FM spins are aligned along the orientation of the external magnetic field (H) and the AFM spins are disordered (Figure 1.1). After cooling the sample below T_N, both FM and AFM spins are aligned along the magnetic field (Figure1.2). In this situation, two limiting cases are possible:

1. For a large AFM anisotropy, shifting of the magnetic hysteresis loop can be observed.
2. For a small AFM anisotropy, a coercivity enhancement (without any loop shift) can be observed.

When the applied magnetic field is reversed in the case of large AFM anisotropy as shown in Figure 1.2, the FM spins begin to rotate and align along the magnetic field and the AFM spins remain fixed for all values of negative H. Due to the strong FM-AFM spin coupling at the interface, an extra amount of magnetic field (and therefore magnetic energy) is required to completely rotate the FM spins. This is manifested in the shift of the hysteresis loop along the negative H field axis.

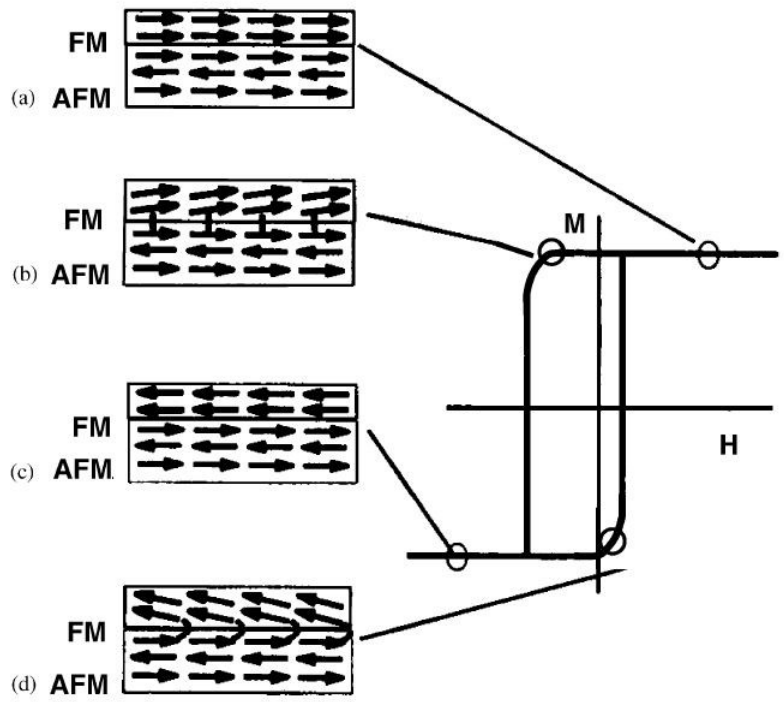

Figure 1.2. The spin configurations of an FM–AFM couple at the different stages of a shifted hysteresis loop for a system [4].

Conversely, the rotation of the FM spins will be easier and will require less magnetic energy to overcome a smaller amount of torque, due to the fixed orientation of the AFM spins at the interface, when the positive magnetic field is applied. Thus, one can observe a shift of the hysteresis loop to smaller positive values than without the exchange bias effect present; the average value of the shift along the positive and negative applied field axes is called the exchange bias field.

On the other hand, both FM and AFM spins are rotated along with magnetic field for a system with small AFM anisotropy (Figure 1.3). As a result, no overall shift of the hysteresis loop is evident in this case. Due to the FM-AFM spin coupling at the interface, a larger magnetic field either for positive or negative values is required to rotate spins. Thus, one can observe an

overall enhancement of the hysteresis loop in case of an interface coupling having a small AFM anisotropy.

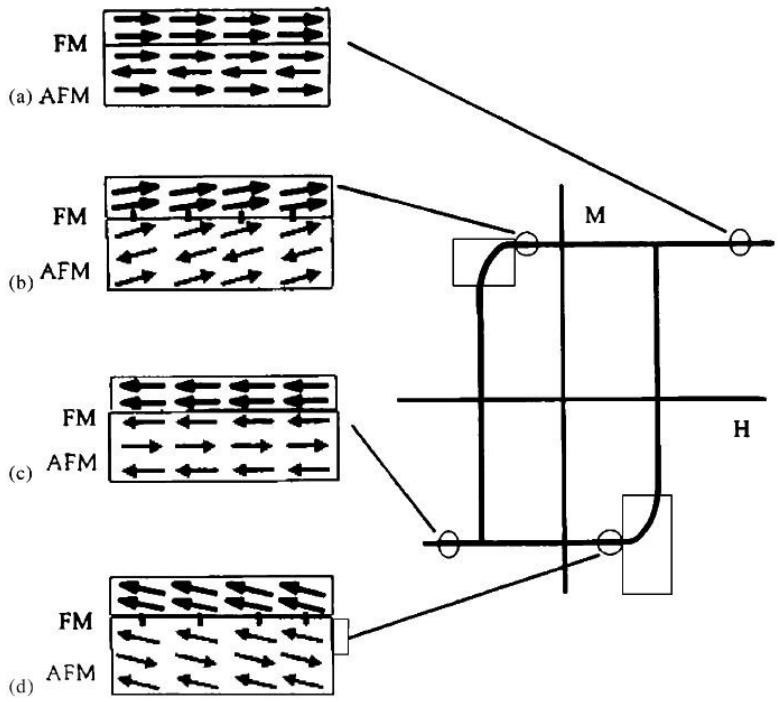

Figure 1.3. The spin configurations of a FM–AFM bilayer, at the different stages for a system with small AFM anisotropy [4].

The exchange bias plays a very important role in the primary components of spintronics devices (spin valves and magnetic tunnel junctions). The primary component structures are similar to the simple model structures shown above but are composed of two FM layers separated by either a non-magnetic metal layer or an insulating/semiconducting AFM layer: in the case of the FM-AFM couple, the exchange bias is used to pin one of the FM layers [6,7,8]. The exchange bias effect is known to originate from the interaction between uncompensated interface spins [4]. However, it most likely also depends upon interface defects (e.g. stacking faults, misfit dislocations, etc.), oxygen vacancies, spin-order disorder effects, and potentially other effects.

The creation and amount of interface defects depend on the nature of synthesis used to make thin film nanostructures, and, in some cases require considerable effort to control.

Nickel oxide (NiO) has the rock salt structure and a Néel temperature of 523 K (in bulk form). This makes it highly useful for room-temperature applications in devices. Bulk NiO is a collinear antiferromagnetic material and its spins are oppositely oriented in alternate (111) crystallographic planes. Thus, bulk NiO exhibits no ferromagnetism and only possesses AFM properties. NiO is a wide band gap semiconductor: however, by introduction of appropriate impurities, it may be possible to narrow the band gap to make it more applicable for semiconductor-based spintronic devices. Thus, for the reasons outlined above, NiO and NiO-based magnetic materials have a very promising role in spintronics based magnetic applications. Based on the previous work made in Dr. Mayanovic's laboratory, it has been shown that Mn and Co can be incorporated to grow NiO@$Mn_xNi_{1-x}O$ and NiO@$Co_xNi_{1-x}O$ core-shell nanoparticles, respectively [9]. This work showed that the $Mn_xNi_{1-x}O$ shell material in particular exhibits substantial ferrimagnetic (FiM) properties, where the FiM phase arises due to having two types of magnetic spins of differing strengths so that only partial cancelation occurs in the case of AFM alignment, and the core shell nanoparticles were shown to exhibit strong exchange bias effects. Furthermore, FM/FiM properties have been observed by introduction of impurity magnetic transition elements in NiO [10].

Thin film epitaxy is preferred for fabrication of thin devices without patterning [11]. This is because for magnetic applications, there is nominal evidence that epitaxial registry at the interface between thin film layers is preferable in order to get a strong exchange bias effect [4]. Nevertheless, there are many techniques that are used to deposit thin film layers, only some of which enable epitaxial deposition. These techniques can be divided into two categories: physical

vapor deposition (PVD) and chemical vapor deposition (CVD) techniques. The pulsed laser deposition (PLD) technique is one of the PVD methods in common use currently and is among the less expensive ones. Molecular beam epitaxy (MBE), which is a PVD method, and atomic layer deposition (ALD), which is a CVD method, are both excellent for fabrication of epitaxial thin film layers but are substantially more expensive for use than PLD. PLD is easier to control compared to other methods, since low process variables (laser power density, substrate target distance and ambient oxygen pressure) are of concern during deposition. Other advantages of PLD are: high deposition rate, high deposition temperature, high partial pressure, easy to couple with in-situ characterization, and versatility in types of materials that can be deposited. Some issues, such as creation of small droplets and deposition on large substrate areas, still need to be dealt with successfully during the PLD process [11].

Figure 1.4 shows the basic principles of the pulsed laser deposition technique in which a laser beam hits the target material. First, the laser generates a plume of material that is projected toward and deposited on the substrate. The substrate is typically placed on a substrate heater to obtain the desired deposition temperature. To create vacuum, different sets of pumps are used. For example, a roughing pump and turbo molecular pump used jointly are capable of creating 10^{-6} to 10^{-8} mbar vacuum. Various types of gas valves are also used to control the gas (O_2, N_2, etc.) flow into the chamber. Moreover, most of the PLD systems have rotating target holders in order to prevent the laser beam from causing damage to the target from over exposure at a select location.

In this study, I wanted to test the hypothesis that nano-sized $Mn_xNi_{1-x}O$ thin films could be grown from a target of nominally similar composition onto NiO thin film layers using the

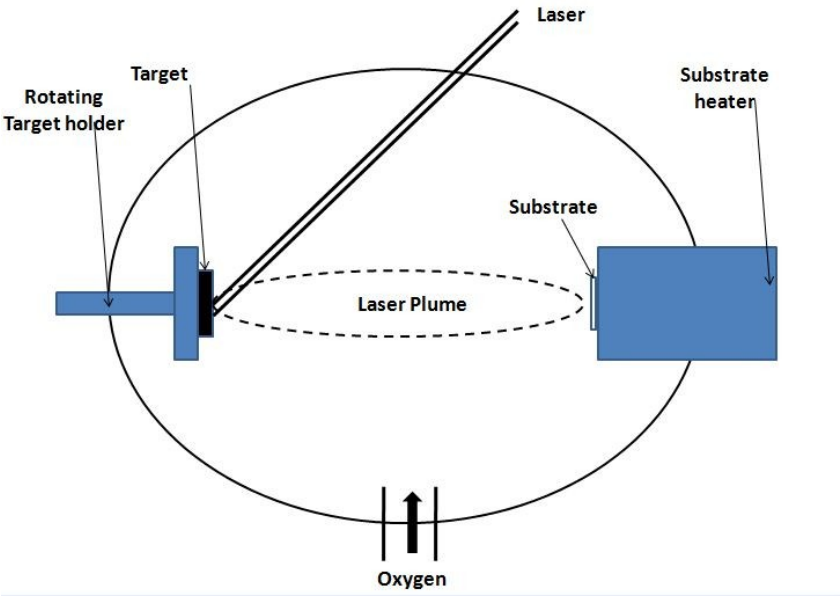

Figure 1.4. Schematic diagram of pulse laser deposition technique.

PLD technique. Indeed, NiO/$Mn_xNi_{1-x}O$ bilayers were successfully deposited on top of MgO and Al_2O_3 substrates by using the PLD technique. Subsequently, XRD and SEM characterization was carried out on the thin film samples, which confirmed the NiO/$Mn_xNi_{1-x}O$ bilayer formation and that these films were grown quasi-epitaxially. Moreover, SQUID magnetometry was carried out on the bilayer samples verifying the AFM/FiM bimagnetic configuration of the thin film heterostructures.

SYNTHESIS AND CHARACTERIZATION OF $NiO/Mn_xNi_{1-x}O$ NANOSCALE HETEROSTRUCTURES GROWN ON MgO (100) SUBSTRATES

Abstract

The exchange bias effect in nanostructured materials has a significant role in the development of high performance spintronics and other spin-related devices. A complete understanding of the exchange bias effect still needs to be elucidated, which can be accomplished by relevant studies undertaken by researchers. In this regard, $NiO/Mn_xNi_{1-x}O$ nanoscale heterostructures were grown on MgO (100) substrates by using the pulsed laser deposition (PLD) technique. The interaction of the spins at the interface between the ferrimagnetic Mn-doped NiO and antiferromagnetic NiO layers triggers the exchange bias effect, which is the primary focus of this investigation. X-ray diffraction (XRD) measurements and scanning electron microscopy (SEM) characterization were made on the $MgO/NiO/Mn_xNi_{1-x}O$ heterostructures. XRD spectra and SEM images showed that $NiO/Mn_xNi_{1-x}O$ thin film layers were grown in the (200) preferred orientation and quasi-epitaxially on top of MgO (100) substrate. Moreover, a desired amount of manganese (Mn) was found to be present in the $Mn_xNi_{1-x}O$ layers of the $MgO/NiO/Mn_xNi_{1-x}O$ heterostructures, as is evident from the SEM-EDX results. Magnetic measurements were also accomplished on the thin film heterostructures using the SQUID magnetometer. The magnetometry results show both an enhancement and a shift of the hysteresis loops due to the exchange bias effect.

Introduction

The importance of bimagnetic nanostructured materials for device related applications is substantial due to considerable progress in controlled synthesis and advanced characterization. These types of nanostructured materials have a wide range of applications in permanent magnets, magnetic recording, microwave absorption, biomedicine, and miniaturized magnetotransport devices [1].

$NiO@Mn_xNi_{1-x}O$ core shell nanoparticles (CSNS), which is just one example of the bimagnetic nanostructured materials, were previously successfully grown and analyzed in Dr. Mayanovic's lab [2]. The main purpose of this study was to determine the role of Mn by substituting for Ni in the NiO-based shell of the resultant CSNS. It was shown from this study that use of the 0.08M concentration precursor $MnCl_2$ led to formation of CSNS with formidable magnetic properties: the hysteresis data showed that at 5K, ~4787Oe coercivity and ~1729Oe exchange bias between FC and ZFC curves were obtained [2].

Bilayer thin film heterostructures are interesting in that the antiferromagnetic (AFM) layer and the ferromagnetic (FM) or ferrimagnetic (FiM) layer share a planar, typically well-oriented interface providing clear evidence of interphase magnetic exchange coupling for specific thin film orientations [3]. This is typically considerably more complicated for bimagnetic heterostructured nanoparticulates because of multiple or lack of distinct orientations between the layers. Thus, $Ni_xM_{1-x}O/NiO$ heterostructures show potential for device fabrication due to substantial exchange interactions evident in the $NiO@Mn_xNi_{1-x}O$ CSNS. Furthermore, it may ultimately be most interesting to exploit the nature of exchange between the substitutional 3d transition metal (TM) in NiO to optimize the magnetic properties of such heterostructured thin films. Given that the superexchange interaction between Ni^{2+} ions is responsible for establishing

AFM ordering in NiO, Zhang et al. showed that a superexchange interaction is established between Ni^{2+} and Fe^{2+} ions, leading to a ferromagnetic interaction between them, in Fe-doped NiO thin films [4]. The hypothesis of this study is that MgO(100)/NiO/$Mn_xNi_{1-x}O$ thin film heterostructures can be fabricated using PLD and that these exhibit magnetic properties consistent with an exchange bias interaction.

Experimental Details

Using pulsed laser deposition (PLD) technique, a NiO thin film layer was first deposited on top of MgO substrates, which were cut and polished on the (100) plane as the deposition surface. The MgO (100) substrates were purchased from the MTI Corporation. Next, the $Mn_xNi_{1-x}O$ thin film layer was deposited using PLD on the NiO layer, resulting in the formation of an MgO(100)/NiO/$Mn_xNi_{1-x}O$ heterostructure. The thin film layers were deposited using a Nd:YAG laser having a wavelength of 266 nm. Table 1 shows the conditions at which MgO/NiO/$Mn_xNi_{1-x}O$ (A) heterostructures were grown within the PLD chamber. Using conditions shown in Table 1, five thin film samples were prepared and characterized using XRD and SEM. From these five samples, the best sample was selected for further characterization. The approximate thickness of the NiO layers varied from 40-70nm and that of the $Mn_xNi_{1-x}O$ layers varied from 20-40nm. For such heterostructures, both the NiO and $Mn_xNi_{1-x}O$ targets were needed be prepared. To prepare the NiO target, NiO nanopowder was mixed with poly vinyl alcohol (PVA). The mixture was ground for two hours. After that, hydraulic pressing was used to make compact shaped circular disk. Finally, the NiO disk was annealed at 1000°C for 2 days. Conversely, the $Mn_xNi_{1-x}O$ target was prepared by mixing $MnCl_2$ powder along with NiO nanopowder and PVA. After grinding and pressing the powder-PVA mixture, a circular disk was formed and finally sintered at 1000°C

for 1 day. SEM-EDX results confirmed that $Mn_xNi_{1-x}O$ target had the desired amount of manganese (~ 4.92 at%). All MgO (100) substrates were single crystal and deposition side was EPI polished; i.e., polished so as to be ready for epitaxial deposition. Prior to deposition of the thin films, the MgO substrates were first cleaned in acetone for 30 minutes and then annealed at 500°C for 2 hours in a high vacuum chamber. The conditions for both layers were the same except for the Q-switch delay. For the NiO layer, a Q-switch delay of 50 was used and for the $Mn_xNi_{1-x}O$ layer, a value of 60 was used. After deposition, both bi-layers were annealed at 500°C for 3 hours in the presence of oxygen gas.

The FESEM (FEI-Quanta 200) instrument was operated at 20 kV for SEM structural and morphological characterization. For imaging purposes, the samples were mounted with copper tape. For elemental analysis, the SEM-EDX was used. The Bruker D8 Discover instrument was used for XRD analysis, with an operating voltage and current of 40 kV and 40 mA, respectively. A characteristic X-ray source Cu tube with a Cu Kα, λ= 1.54184 Å was used for XRD measurements. The SQUID MPMS/XL magnetometer (Quantum Design, USA) was used to measure magnetic properties of the thin films. Capsules were used to pack the samples and then inserted into the SQUID magnetometer. The magnetization (M) vs temperature (T) data were measured in the 5 – 300 K. A 300 Oe applied field was used to freeze the spins for the field-cooled (FC) magnetization vs temperature (M-T) data and the same field was used to measure both the FC and zero-field-cooled (ZFC) M-T data. Magnetic hysteresis curve measurements were measured from -6 to +6 KOe at 5K and at 300K.

Table 1. Deposition parameters for MgO/NiO/$Mn_xNi_{1-x}O$ (A) heterostructures.

	NiO Deposition			$Mn_xNi_{1-x}O$ Deposition		
Name	Temperature	Pressure	Pulses	Temperature	Pressure	Pulses
A	500 °C	2.4e-2 mbar O^2	40,000	500 °C	2.4e-2 mbar O^2	40,000

Results & Discussion

Figure 2.1 shows the short range (2-theta; 42-45°) of the XRD scan containing the (200) peaks and measured from the a) MgO/NiO substrate and thin film layer and from the b) MgO/NiO/$Mn_xNi_{1-x}O$ heterostructure. Both MgO and NiO have the rock salt structure with space group $Fm\bar{3}m$. For the MgO/NiO substrate-thin film arrangement, the lattice mismatch between the film and substrate is 0.254% and the corresponding lattice constant of the NiO thin film is 4.1792Å, as determined using Bragg's Law. On the other hand, for the MgO/NiO/$Mn_xNi_{1-x}O$ heterostructure, the lattice mismatch between the NiO/$Mn_xNi_{1-x}O$ combined layers and the MgO substrate was found to be 0.245% and the corresponding lattice constant for the former is 4.1796 Å. Due to the presence of manganese, the lattice constant for the MgO/NiO/$Mn_xNi_{1-x}O$ heterostructure is larger than that of the MgO/NiO heterostructure. Note that it is not possible to resolve the NiO vs $Mn_xNi_{1-x}O$ layer lattice constant because of the preferred orientation of the layers and having limited peaks in the XRD patterns.

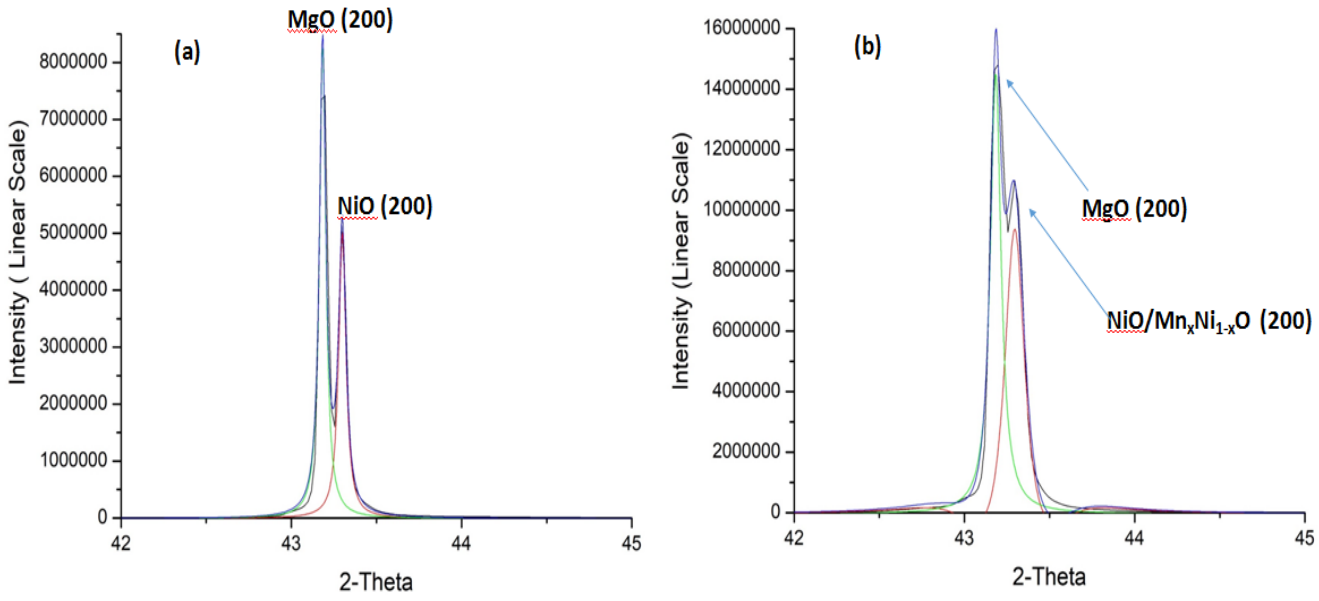

Figure 2.1. Short range (2-theta; 42-45°) XRD scan measured from the a) MgO/NiO b) MgO/NiO/$Mn_xNi_{1-x}O$ heterostructures.

Figure 2.2 shows an extended-range (2-theta; 20-105°) XRD scan for the MgO/NiO/$Mn_xNi_{1-x}O$ heterostructure. In the lower 2-theta range (40-50°), there is a single peak having various components. This is partially due to the fact that the overall peak has two contributions (as observed from the high resolution spectrum shown above); one is from the MgO substrate and other is from the NiO/$Mn_xNi_{1-x}O$ bi-layers [5]. At the higher 2-theta range (90-105°) in the XRD spectrum shown in Figure 2.2, we see a similar peak convolution in the overall peak shape but in this case, it is evident that the peaks from the NiO/$Mn_xNi_{1-x}O$ bi-layers and from the MgO substrate are resolved. Additionally, it is evident from the peak shape in both the low and higher 2-theta peaks that the MgO/NiO/$Mn_xNi_{1-x}O$ thin film heterostructure has both crystalline and amorphous portions. The sharp peak features provide evidence for crystallinity whereas the wide sections near the bottom of the peaks, particularly the shoulder appearing on the high 2-theta side, provide evidence for the amorphous component.

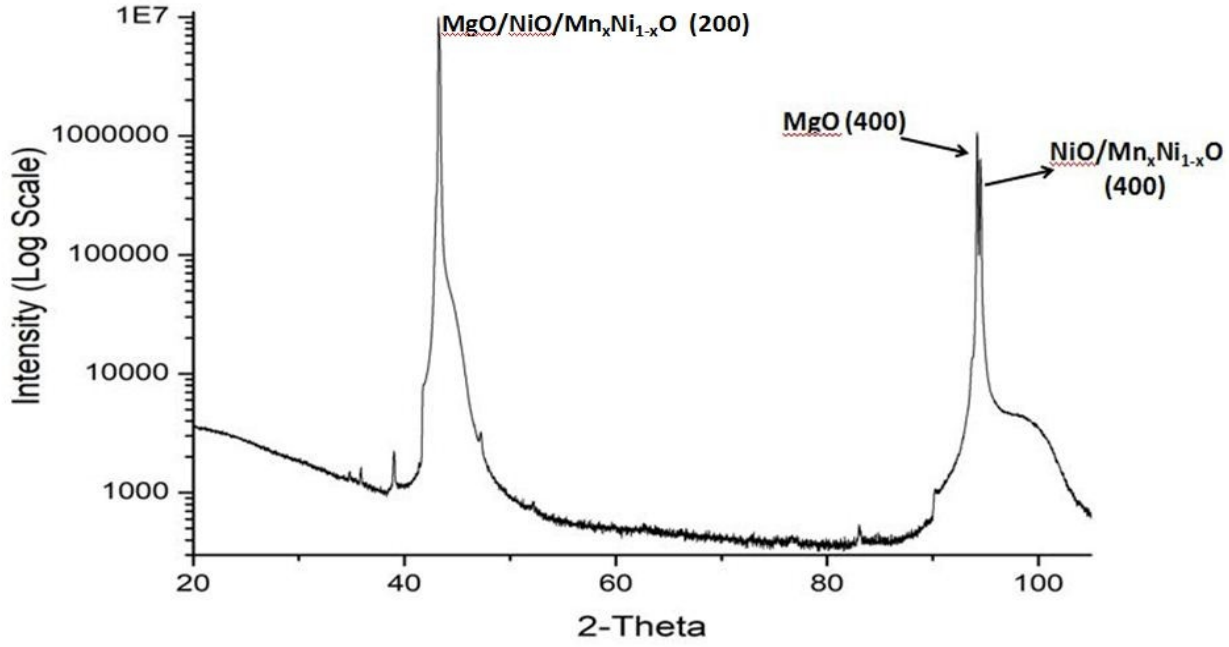

Figure 2.2. Long range (2-theta; 20-105°) XRD scan measured from the MgO/NiO/$Mn_xNi_{1-x}O$ thin film heterostructure.

Figure 2.3 shows the SEM and SEM-EDX results (SEM micrograph, EDX spectrum & quantitative data; clockwise) for the $Mn_xNi_{1-x}O$ target. The SEM micrograph shows the compactness of the $Mn_xNi_{1-x}O$ target, due to the agglomeration of the fine powder particles. Manganese peaks can be seen in the EDX spectrum shown in Figure 2.3, indicating that manganese was successfully incorporated into the $Mn_xNi_{1-x}O$ target. Quantitative SEM-EDX analysis shows that 4.92 atomic percent (at%) manganese, 42.93 at% nickel and 52.15 at% oxygen are present in the target.

Figure 2.4 shows the SEM micrograph, EDX spectrum and SEM-EDX quantitative data (clockwise) for the MgO/NiO/$Mn_xNi_{1-x}O$ heterostructure that was selected for the full characterization. From the SEM micrograph, it is evident that the thin film bi-layers are smooth in places but granular in others. The granular (blob) like regions occur from droplets of plasma

material being deposited in select location on either the substrate, or in case of the $Mn_xNi_{1-x}O$ thin film, on the NiO layer. Due to the relatively large amount of localized material in the

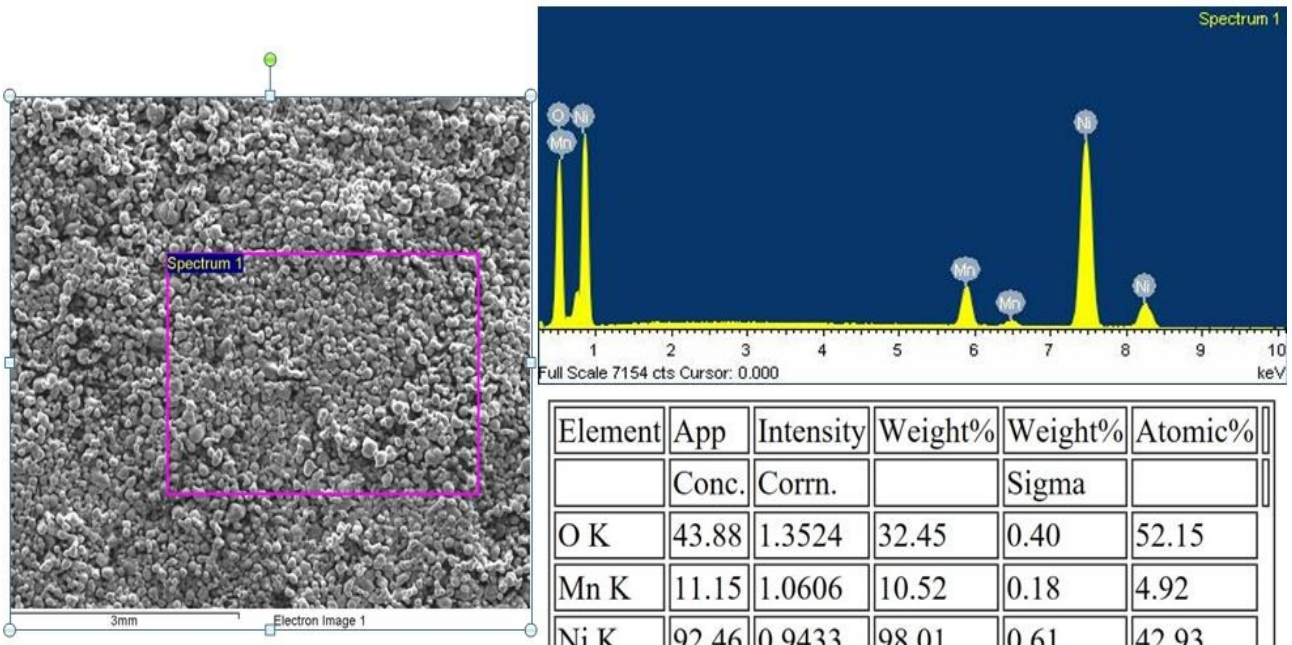

Element	App Conc.	Intensity Corrn.	Weight%	Weight% Sigma	Atomic%
O K	43.88	1.3524	32.45	0.40	52.15
Mn K	11.15	1.0606	10.52	0.18	4.92
Ni K	92.46	0.9433	98.01	0.61	42.93
Totals			140.98		

Figure 2.3. SEM micrograph (left) and SEM-EDX (right) spectrum of the $Mn_xNi_{1-x}O$ target.

droplets, the atomic diffusion during deposition is insufficient in distributing the material laterally on the depositing surface resulting in the blob-like appearance. Thus, because the deposition during PLD is somewhat but not completely controlled on an atom-by-atom basis, it is reasonable that the films should exhibit both crystalline/epitaxial and amorphous/disordered characteristics. The EDX spectrum shows that a nominal amount of manganese (0.13 at%) is present in the heterostructure, with the remaining content being nickel, oxygen and magnesium.

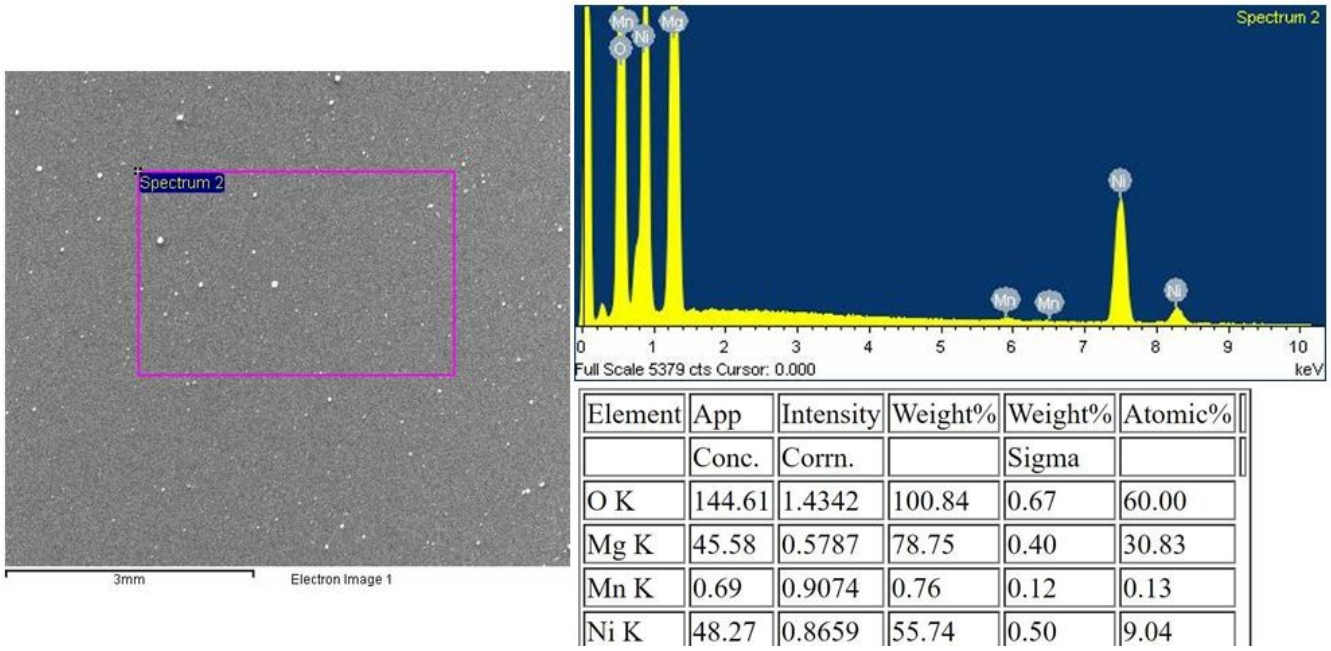

Element	App Conc.	Intensity Corrn.	Weight%	Weight% Sigma	Atomic%
O K	144.61	1.4342	100.84	0.67	60.00
Mg K	45.58	0.5787	78.75	0.40	30.83
Mn K	0.69	0.9074	0.76	0.12	0.13
Ni K	48.27	0.8659	55.74	0.50	9.04

Figure 2.4. SEM micrograph (left) and SEM-EDX (right) spectrum of the MgO/NiO/$Mn_xNi_{1-x}O$ heterostructure.

Full magnetization characterization using the SQUID PPMS was made on the select MgO/NiO/$Mn_xNi_{1-x}O$ thin film heterostructure sample. The magnetization vs applied field (M vs H) data measured from the MgO/NiO/$Mn_xNi_{1-x}O$ heterostructure at 5 K and at 300K are shown in Figure 2.5. As can be seen, the magnetization of the heterostructure increases rapidly with the increasing field and clearly reaches a saturation value. The standard "S" shape of the hysteresis curves is indicative of either FM or FiM character of the $Mn_xNi_{1-x}O$ layer; the NiO is AFM and typically exhibits only paramagnetic like characteristics in M vs H curves. The coercivity values, where M = 0 for negative (or positive) applied field, for zero-field cooled (ZFC) and field cooled (FC) hysteresis curves are as follows: for the ZFC case, the coercivity is 114 Oe and for the FC case, the coercivity is 186 Oe at 5 K. Conversely, the coercivity values for ZFC and FC are the same, specifically 62 Oe at 300K. Hasan et al. have established from DFT based calculations that

the rock salt structured $Mn_xNi_{1-x}O$ phase has FiM properties [6]. Thus, we conclude that due to the presence of Mn, FiM ordering has been observed in the $MgO/NiO/Mn_xNi_{1-x}O$ heterostructure [2]. In the exchange bias effect for a bimagnetic heterostructured system having a relatively large AFM anisotropy, the hysteresis loops shift either in the negative (FC) or positive (ZFC) H axis direction. The exchange bias field He values were calculated using the following expression: $He = (H_{ZFC+} - H_{FC+} - H_{FC-} + H_{ZFC-})/2$, where the +/- signs stand for positive/negative H values when M=0 [2]. Thus, for the $MgO/NiO/Mn_xNi_{1-x}O$ heterostructure at 5K, the value of the exchange bias is ~33Oe. On the other hand, as the ZFC and FC hysteresis loops have essentially identical coercivities at 300K, the exchange bias effect is not evident under room temperature conditions. This is fairly typical for most magnetic materials unless they have very high magnetic anisotropies that persist to room temperature conditions. Otherwise, the random thermal fluctuations at ambient conditions disrupt the pinning of the uncompensated $NiO\text{-}Mn_xNi_{1-x}O$ interface spins that are thought to be responsible for the exchange bias effect. The relatively small He field value measured at 5 K is consistent with the lack of full epitaxy and presence of substantial disorder at the $NiO\text{-}Mn_xNi_{1-x}O$ interface, as is evident from the XRD results. A relatively high level of crystallinity is required to establish a high degree of pinning of the uncompensated spins at the $NiO\text{-}Mn_xNi_{1-x}O$ interface. Nevertheless, the most interesting feature is that the FiM properties of the $Mn_xNi_{1-x}O$ thin film layer persist to room temperature, as evidenced by the hysteresis loops measured at 300K. This is an important development for potential future practical applications of bimagnetic $NiO/Mn_xNi_{1-x}O$ thin film heterostructures since devices using such materials are expected to operate at room temperature conditions.

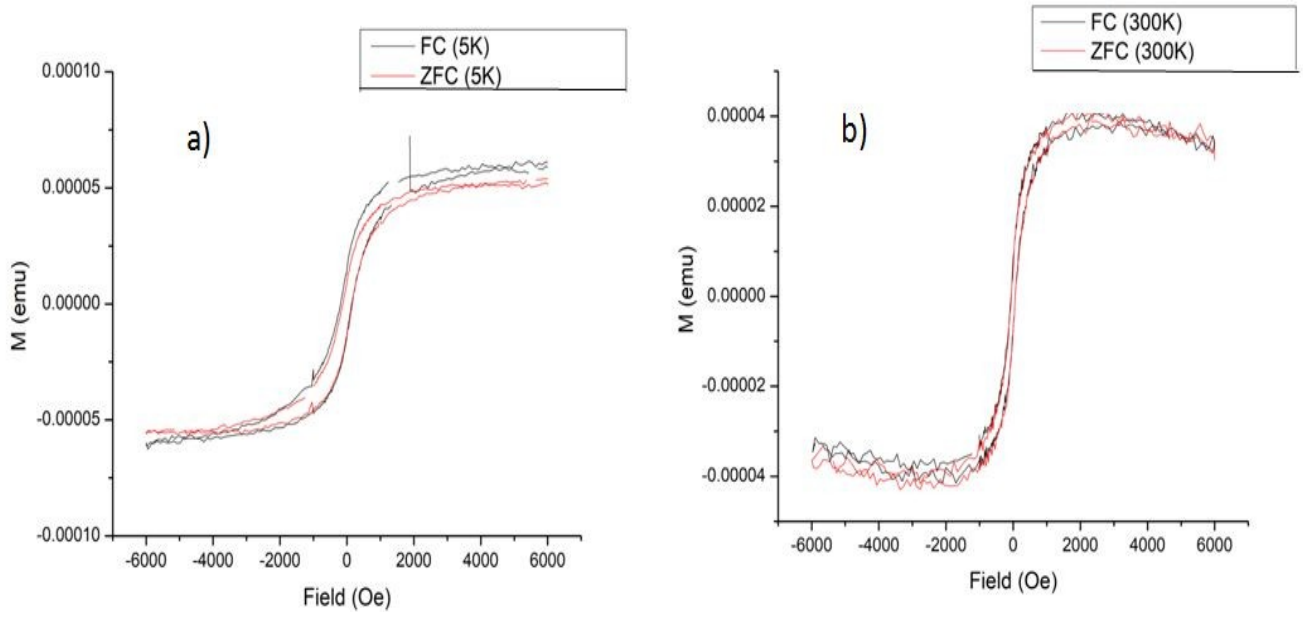

Figure 2.5. The zero field cooled (ZFC) and field cooled (FC) magnetization vs applied field (M vs H) data measured from the MgO/NiO/$Mn_xNi_{1-x}O$ heterostructureat a) 5 K and b) 300K.

Figure 2.5 a) also shows a vertical shift (i.e., along the M axis) of the FC hysteresis curve, relative to the ZFC curve, from the M vs H measurements made at 5 K of the MgO/NiO/$Mn_xNi_{1-x}O$ thin film heterostructure sample. The vertical shift is attributed to the frozen Ni spins (at 5 K) at the NiO-$Mn_xNi_{1-x}O$ interface stemming from the NiO layer. The frozen Ni spins that may act like those in a spin glass system and originate from disorder effects at the interface, such as misfit dislocations, vacancies, stacking faults, strain effects, etc. This is consistent with our XRD results showing nominal disorder/amorphous like features attributed to the MgO/NiO/$Mn_xNi_{1-x}O$ thin film heterostructure.

Conclusions

In conclusion, NiO and $Mn_xNi_{1-x}O$ bi-layers were grown quasi-epitaxially on MgO (100) substrates in the presence of oxygen. The MgO (200) and NiO/$Mn_xNi_{1-x}O$ (200) planes are parallel to each other as confirmed from XRD measurements. XRD results also confirm that

$NiO/Mn_xNi_{1-x}O$ thin film bi-layers have both crystalline and disordered and/or amorphous components. The SEM-EDX results confirm the presence of Mn in the $MgO/NiO/Mn_xNi_{1-x}O$ thin film heterostructure. SQUID magnetometry of the thin film heterostructure showed that a weak exchange bias (He = 33 Oe) persists at 5 K but that there is no exchange bias present at room temperature. Furthermore, the magnetic data are consistent with the $Mn_xNi_{1-x}O$ thin film layer of the heterostructure having FiM magnetic properties. Interestingly, the SQUID magnetometry data show that the FiM magnetism persists to room temperature. The magnetometry and XRD results are consistent with appreciable structural disorder at the NiO-$Mn_xNi_{1-x}O$ interface.

References

[1] A. López-Ortega, M. Estrader, G. Salazar-Alvarez, A.G. Roca, and J. Nogués, Phys. Rep. **553**, 1 (2015).

[2] S. Hasan, MSU Grad. Theses (2017).

[3] K.-W. Lin, R.J. Gambino, and L.H. Lewis, J. Appl. Phys. **93**, 6590 (2003).

[4] Y.-J. Zhang, Y.-D. Luo, Y.-H. Lin, and C.-W. Nan, Appl. Phys. Lett. **104**, 072402 (2014).

[5] Y. Kokubun, Y. Amano, Y. Meguro, and S. Nakagomi, Thin Solid Films **601**, 76 (2016).

[6] S. Hasan, R.A. Mayanovic, and M. Benamara, MRS Adv. **2**, 3465 (2017).

SYNTHESIS AND CHARACTERIZATION OF $NiO/Mn_xNi_{1-x}O$ NANOSCALE HETEROSTRUCTURES GROWN ON Al_2O_3 (111) SUBSTRATES

Abstract

The exchange bias (EB) effect is especially useful in nanomaterials and shows promise for antiferromagnet-based spintronics applications. It is well established that antiferromagnetic characteristics of conventional NiO insulating material can be altered to ferromagnetic or ferrimagnetic characteristics by substitution with 3d transition elements. In this work, I have used the pulsed laser deposition (PLD) technique to develop quasi-epitaxial heterostructures on the (111) surface of the Al_2O_3 substrate. For quasi-epitaxial heterostructures, a ferrimagnetic $Mn_xNi_{1-x}O$ thin film layer was interfaced with an antiferromagnetic NiO thin film layer, which was first deposited on the Al_2O_3 substrate. X-ray diffraction (XRD) and scanning electron microscope (SEM) were carried out on the $Al_2O_3/NiO/Mn_xNi_{1-x}O$ heterostructures. The XRD and SEM results show that the $Mn_xNi_{1-x}O$ and NiO layers were grown quasi-epitaxially on the (111) surface of the Al_2O_3 substrate. Incorporation of Mn in the $Mn_xNi_{1-x}O$ layer was confirmed by using SEM energy dispersive spectroscopy (SEM-EDX). The magnetic properties of a select $Al_2O_3/NiO/Mn_xNi_{1-x}O$ heterostructure were analyzed using SQUID magnetometry.

Introduction

The exchange bias (EB) effect, which is a fundamental magnetic interfacial property has immense technical importance for magneto-electronic device applications [1]. The EB effect was discovered more than fifty years ago by Meiklejohn and Bean [3]. After decades of experimental and theoretical studies, the common acceptable theory of exchange bias is due to the spin-spin

coupling occurring at the interface between ferromagnetic (FM), or ferrimagnetic (FiM), and antiferromagnetic (AFM) layers. The exchange bias effect has been studied in a number of different systems; however, the most common systems are core-shell nanoparticles and layered thin films [4].

For device applications, the dominant type of substrate used is the corundum-structured aluminum oxide (α-Al_2O_3): for the sake of simplicity, I will refer to this simply as alumina or Al_2O_3. Existing industry expertise enables high availability of low-cost alumina, which is particularly important for inexpensive production of light emitting devices (LEDs). This provides for alumina having high resistivity, good mechanical and dielectric strength, and excellent thermal and corrosion stability. These qualities also provide for some disadvantages; however, none of these are too serious for the intended magnetic applications. The two most obvious disadvantages of using alumina are the inefficiency to propagate electrical signal and draw heat away from the device [5].

NiO is a conventional antiferromagnetic (AFM) material. Its AFM spins in the adjacent {111} planes align in the opposite direction [2]. NiO is particularly desirable for use in bimagnetic heterostructured-based devices because its Néel temperature (in bulk form) is ~525 K (~252 °C), thus making it practical for room-temperature use. Previous studies have shown that NiO can be grown along its (111) crystallographic (planes) orientation on the Al_2O_3 substrate oriented along its (0001) planes (i.e., NiO (111) on Al_2O_3(0001)) [6]. Thus, with this oriented growth and perfect crystallinity, NiO AFM spins are parallel to the Al_2O_3 [0001] orientation. Moreover, in the ideal case with perfect crystallinity, when NiO/$Mn_xNi_{1-x}O$ bilayers are grown on the top of Al_2O_3 (0001) surface, the coupling between FiM ($Mn_xNi_{1-x}O$) and AFM (NiO) spins should be stronger when compared to the coupling of FiM/AFM spins and enabling the exchange bias effect in

$NiO@Mn_xNi_{1-x}O$ core-shell nanoparticles. This is because of the canting effect of the spins, which is expected to be present in $NiO@Mn_xNi_{1-x}O$ core-shell nanoparticles having pseudospherical morphology, should be absent in ideal, well oriented thin film interfaces. Strong coupling between FM and AFM spins should enable a strong exchange bias effect and, potentially a perpendicular exchange bias effect where the spins couple in perpendicular orientation as opposed to parallel orientation. Because PLD does not enable perfect epitaxial growth (i.e., close to ideal crystallinity) of thin films, such as the atomic layer deposition (ALD) technique does, very strong exchange bias and magnetic properties for $NiO/Mn_xNi_{1-x}O$ bilayers grown on the top of the Al_2O_3 (0001) surface are not expected. Conversely, PLD is a much less expensive and practical technique to use then, for example, ALD for the potential fabrication of $NiO/Mn_xNi_{1-x}O$ bilayer-based devices in industry. Thus, the primary hypothesis of my study is to investigate whether $NiO/Mn_xNi_{1-x}O$ nanostructured bilayers grown on Al_2O_3 (0001) using PLD can produce favorable magnetic properties, including the exchange bias effect, for use in magnetic devices.

Experimental Details

Pulsed laser deposition (PLD) technique was used to create $Al_2O_3(0001)/NiO/Mn_xNi_{1-x}O$ heterostructures for this study. First, a NiO thin film layer was deposited on top of commercially purchased $Al_2O_3(0001)$ substrates. Next, the $Mn_xNi_{1-x}O$ thin film layer was deposited on the top of NiO layer. A Nd:YAG laser having a wavelength of 266 nm was used for the PLD deposition. The following procedures were used to grow the thin film layers. First, the vacuum chamber was cleaned properly. Subsequently, targets were placed in the target holders inside the growth chamber: the fabrication of the NiO and $Mn_xNi_{1-x}O$ was described in Chapter 2. Next, the

substrate holder was cleaned using isopropanol alcohol whereas the Al_2O_3 (0001) substrate was cleaned using acetone and sonication for 30 minutes. Next, the substrate was placed in the substrate holder inside the PLD growth chamber. After that, 1.0e-5 mbar vacuum was created using rotary and turbo molecular pumps. Prior to deposition, the substrate heater was used to anneal the substrate at 500°C for 2 hours. Except for the Q-switch delay, identical conditions were used for both thin film layers. For NiO and $Mn_xNi_{1-x}O$ layers, a Q-switch delay of 50 and 60 were used, respectively. Both thin film layers were deposited at 500°C in the presence of 1.8e-2 mbar O_2 partial pressure, a laser repetition rate of 10 Hz and a fixed amount of 40,000 shots were used. After deposition, Al_2O_3(0001)/NiO/$Mn_xNi_{1-x}O$ heterostructures were annealed at 500°C for 3 hours in the presence of oxygen gas. Using the above mentioned conditions, a total of three samples were prepared and characterized using XRD and SEM. The thin film Al_2O_3(0001)/NiO/$Mn_xNi_{1-x}O$ heterostructure having the best structural, morphological and constitutional properties was used for further characterization. The approximate thickness of the NiO layers varied from 50-65nm and of the $Mn_xNi_{1-x}O$layers from 30-40nm.

Results & Discussion

The long range (2-theta; 20-85°) XRD scan measured from the Al_2O_3/NiO/$Mn_xNi_{1-x}O$ thin film heterostructure (i.e., the sample selected for an extensive characterization) is shown in Figure 3.1. It is clear from the XRD spectrum that the NiO/$Mn_xNi_{1-x}O$ thin film bilayers were grown along the (111) crystallographic orientation on top of the Al_2O_3 (0001) substrate. The overall peak at lower 2-theta range (35-40°) is due to the NiO/$Mn_xNi_{1-x}O$ (111) crystallographic planes of the thin film bilayers, the one in the middle 2-theta range (40-45°) is due to the Al_2O_3 (0001) substrate and the overall higher 2-theta range (77-80°) peak is due to the NiO/$Mn_xNi_{1-x}O$

(222) crystallographic planes. Moreover, all three peaks contain predominantly crystalline features with a small amount of amorphous portions. The sharp and narrow portions are attributed to the crystalline features whereas the widening at the bottom is attributed to the disordered or amorphous components. Thus, the $Al_2O_3/NiO/Mn_xNi_{1-x}O$ thin film heterostructure is predominantly crystalline.

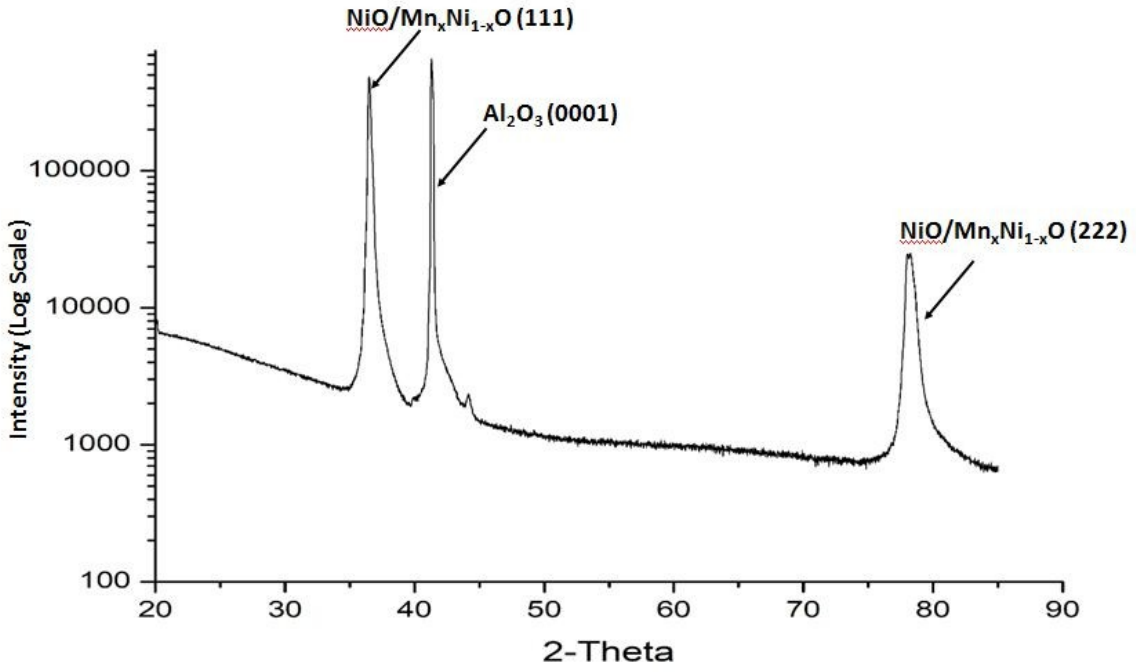

Figure 3.1. An XRD scan measured from the $Al_2O_3/NiO/Mn_xNi_{1-x}O$ thin film heterostructure.

Figure 3.2 shows the SEM micrograph, the EDX spectrum and quantitative data for the $Al_2O_3/NiO/Mn_xNi_{1-x}O$ heterostructure that was selected for full characterization. It is clear from the SEM micrograph that the thin film bilayers have both mostly smooth and small granular, blob-like regions. The occurrence of granular (blob) like regions is due to droplets of plasma material being deposited on either the substrate, or on the NiO layer having relatively large amount of localized material and insufficient lateral atomic diffusion during deposition. Thus,

completely controlled atom-by-atom basis deposition is not possible during PLD deposition; it is obvious that the NiO and $Mn_xNi_{1-x}O$ films have both crystalline/epitaxial and amorphous/disordered characteristics.

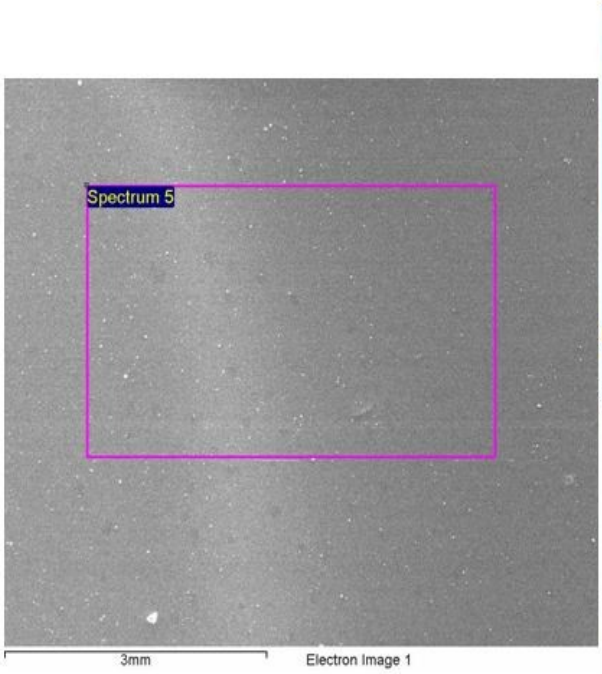

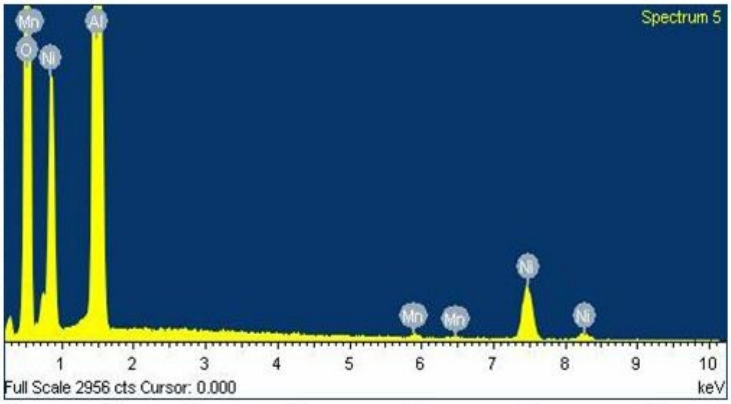

Element	App Conc.	Intensity Corrn.	Weight%	Weight% Sigma	Atomic%
O K	97.50	1.2481	78.12	0.61	67.39
Al K	47.89	0.8241	58.11	0.27	29.73
Mn K	0.35	0.8465	0.41	0.08	0.10
Ni K	10.05	0.8498	11.83	0.25	2.78
Totals			148.47		

Figure 3.2. An SEM micrograph (left) of and the SEM-EDX (right) spectrum measured from the $Al_2O_3/NiO/Mn_xNi_{1-x}O$ heterostructure.

However, the predominant features in the SEM micrograph film are comprised of the smooth regions which are crystalline/epitaxial in nature. This is consistent with the XRD results. The EDX spectrum shows that a significant amount of manganese is present in the heterostructure, at a quantity of 0.10 at%, whereas the nickel, oxygen and aluminum compositions are 2.78, 67.39, and 29.73 at%, respectively.

After subtracting the diamagnetic contribution stemming from the substrate, the magnetization vs applied field (M vs H) data measured in the zero field (ZFC) and field cooled

(FC) condition from the $Al_2O_3/NiO/Mn_xNi_{1-x}O$ heterostructure, that was selected for full magnetization characterization, using the SQUID PPMS at 5 K (left) and at 300K (right), are shown in Figure 3.3. From Figure 3.3, it is clearly evident that the magnetization of the heterostructure increases rapidly with the increase of the applied field H. Moreover, the magnetization vs applied field clearly reaches a saturation value and has a standard "S" shape in all cases. The standard "S" shape of the hysteresis curves indicates that the $Mn_xNi_{1-x}O$ layer in the heterostructure has FM or FiM characteristics. On the other hand, the NiO layer in the heterostructure has AFM characteristic due to the presence of a small but nevertheless paramagnetic like characteristic in the M vs H curves. By definition, the coercivity is the value of the reverse magnetic field required to make the magnetization zero (M= 0). For the ZFC case, the coercivity is 250 Oe and for the FC case, the coercivity is 370 Oe as measured at 5 K. Moreover, for the ZFC case, the coercivity is 150 Oe and for the FC case, the coercivity is 200 Oe as measured at 300K. From the Hasan et al. study using DFT based calculations and our magnetic results, I conclude that $Mn_xNi_{1-x}O$ phase has FiM properties in the $MgO/NiO/Mn_xNi_{1-x}O$ heterostructure due to presence of Mn [1,7]. The exchange bias effect is the shift of the hysteresis loop either in the positive or negative applied field direction. In the case of the $NiO/Mn_xNi_{1-x}O$ bilayer, the shift occurs due to the stronger AFM anisotropy of the NiO layer, as compared to the FiM anisotropy of the $Mn_xNi_{1-x}O$ layer. The value of the exchange bias field can be calculated using the formula $H_E = (H_{ZFC+} - H_{FC+} - H_{FC-} + H_{ZFC-})/2$, where the +/- signs indicate positive/negative coercivity values. Thus, for the $Al_2O_3/NiO/Mn_xNi_{1-x}O$ heterostructure measured at 5K, the value of the exchange bias field is ~70Oe. Furthermore, the value of the exchange bias for the heterostructure at 300 K is ~19 Oe. The most notable aspect is that the exchange bias, although small, is nevertheless observable at room temperature for the

Al_2O_3/NiO/$Mn_xNi_{1-x}O$ heterostructure. The implications of this are that sufficiently strong NiO AFM anisotropy, along with FiM ordering, persist at room temperature resulting in the pinning of the uncompensated Ni and Mn spins at the NiO-$Mn_xNi_{1-x}O$ interface. The relatively small values for the coercivity and exchange bias is most likely due to that fact that the NiO/$Mn_xNi_{1-x}O$ thin film bilayers are not fully epitaxial and contain disordered regions. Although the crystalline components predominate throughout the NiO and $Mn_xNi_{1-x}O$ layers, the magnetization results are consistent with significant (proportionally) disordered regions at the NiO-$Mn_xNi_{1-x}O$ interface. The vertical shift at both temperature (5K and 300K) is attributed to the frozen Ni spins at the NiO-$Mn_xNi_{1-x}O$ interface, which most likely originate from the disordered regions of the interface. The vertical shift occurs because the orientation of the frozen Ni surface spins is in the same direction as the positive applied field, in the FC case, and these remain fixed (i.e., cannot be flipped) when the H field is reversed in the opposite direction.

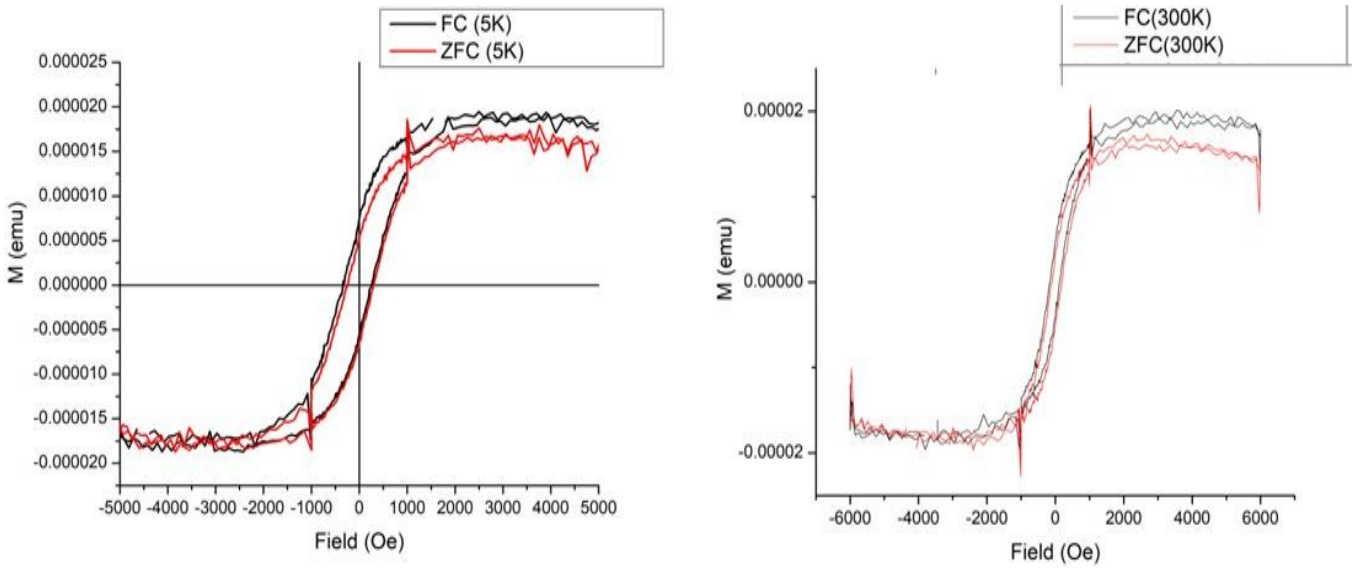

Figure 3.3. The magnetization vs applied field (M vs H) data measured in the zero field cooled (ZFC) and field cooled (FC) conditions from the Al_2O_3/NiO/$Mn_xNi_{1-x}O$ heterostructureat 5 K (left) and 300K (right).

Conclusions

The XRD results show that the $NiO/Mn_xNi_{1-x}O$ bi-layers were grown along the (111) crystallographic planes oriented on top of Al_2O_3 (0001) substrate. From the SEM micrographs, it is evident that both thin film bi-layers have mostly smooth regions with smaller granular regions. The XRD and SEM data are consistent with the $NiO/Mn_xNi_{1-x}O$ thin film bi-layers being predominantly crystalline and containing lesser regions that are disordered and/or amorphous. Thus, the $NiO/Mn_xNi_{1-x}O$ thin film bi-layers were grown quasi-epitaxially on Al_2O_3 (0001) substrates in the presence of oxygen using the PLD technique. An extensive magnetic characterization, in terms of measurement of hysteresis curves in the FC and ZFC case, was made on a select $Al_2O_3/NiO/Mn_xNi_{1-x}O$ heterostructure at 5 K and 300 K. The magnetization data reveal that the exchange bias field is ~70Oe when measured at 5 K and ~19Oe when measured at 300 K. A vertical shift is observed between the FC and ZFC hysteresis curves for measurements made at 5 K and 300 K. The vertical shift is attributed to frozen Ni spins near the $NiO\text{-}Mn_xNi_{1-x}O$ interface of the heterostructure. The observed exchange bias effect at room-temperature indicates that the FiM ordering of the $Mn_xNi_{1-x}O$ thin film and the AFM anisotropy of the NiO thin film, observed for an $Al_2O_3/NiO/Mn_xNi_{1-x}O$ heterostructure, also persist to room temperature and can potentially be useful for room temperature device applications.

References

[1] S. Hasan, MSU Grad. Theses (2017).

[2] K. Arai, T. Okuda, A. Tanaka, M. Kotsugi, K. Fukumoto, T. Ohkochi, T. Nakamura, T. Matsushita, T. Muro, M. Oura, Y. Senba, H. Ohashi, A. Kakizaki, C. Mitsumata, and T. Kinoshita, Phys. Rev. B **85**, 104418 (2012).

[3] F. Radu and H. Zabel, in *Magn. Heterostruct. Adv. Perspect. Spinstructures Spintransport*, edited by H. Zabel and S.D. Bader (Springer, Berlin, Heidelberg, 2008), pp. 97–184.

[4] Z. Leuty, MSU Grad. Theses (2018).

[5]Encycl. Br. (n.d.).

[6] K. Uchida, K. Yoshida, D. Zhang, A. Koizumi, and S. Nozaki, AIP Adv. **2**, 042154 (2012).

[7] S. Hasan, R.A. Mayanovic, and M. Benamara, MRS Adv. **2**, 3465 (2017).

SUMMARY

In my thesis project, I have made a structural, morphological and magnetic study of $MgO/NiO/Mn_xNi_{1-x}O$ and $Al_2O_3/NiO/Mn_xNi_{1-x}O$ thin film heterostructures. From the XRD results, it is evident that the NiO and $Mn_xNi_{1-x}O$ thin film bilayers were grown along the (200) crystallographic plane orientation on top of the MgO (100) substrate and (111) crystallographic plane orientation on top of the Al_2O_3 (0001) substrate. XRD results also confirm that both heterostructures contain crystalline/epitaxial and amorphous/disorder portions. However, XRD results also show that the $Al_2O_3/NiO/Mn_xNi_{1-x}O$ heterostructure has greater crystallinity than the $MgO/NiO/Mn_xNi_{1-x}O$ heterostructure. This is most likely due to a higher level of crystallinity of the Al_2O_3 (0001) substrates compared to that of the MgO (100) substrates that were used in this study. SEM micrographs show that both heterostructures have smooth and granular regions. From the SEM micrographs, it is also clear that $Al_2O_3/NiO/Mn_xNi_{1-x}O$ thin film heterostructure is smoother compared to the $MgO/NiO/Mn_xNi_{1-x}O$ heterostructure. Thus, the $Al_2O_3/NiO/Mn_xNi_{1-x}O$ thin film heterostructure is more epitaxial and has less disordered regions, which is consistent with the XRD results. Moreover, magnetic hysteresis results confirm that both heterostructures exhibit room temperature FiM properties, which can be useful for spintronics and other magnetic based device applications. Furthermore, both heterostructures show large AFM anisotropies and corresponding exchange bias effects at 5K. Nonetheless, the $Al_2O_3/NiO/Mn_xNi_{1-x}O$ heterostructure was found to possess a significant AFM anisotropy, FiM magnetization and corresponding exchange bias effect at room temperature. The coercivity and exchange bias field values are higher for the $Al_2O_3/NiO/Mn_xNi_{1-x}O$ thin film heterostructure compared to that of the $MgO/NiO/Mn_xNi_{1-x}O$ thin film heterostructure at 5 K. This is due to the fact that

Al_2O_3/NiO/$Mn_xNi_{1-x}O$ thin film heterostructure is more epitaxial/crystalline and has more regions of good interface matching compared to that of the MgO/NiO/$Mn_xNi_{1-x}O$ thin film heterostructure. For the MgO/NiO/$Mn_xNi_{1-x}O$ thin film heterostructure, a vertical shift (i.e., along the M axis) of the FC hysteresis curve relative to the ZFC curve was found to occur at 5K but not at 300 K. Conversely, the vertical shift of the FC hysteresis curve along the M axis relative to the ZFC curve occurred at both 5K and 300K for Al_2O_3/NiO/$Mn_xNi_{1-x}O$ thin film heterostructure. The vertical shift of hysteresis loop is attributed to the frozen Ni spin-glass-like spins at the interface between the NiO and $Mn_xNi_{1-x}O$ thin film layers.

REFERENCES

[1] B. Cord, W. Maass, J. Schroeder, K.-H. Schuller, and U. Patz, Thin Solid Films **175**, 287 (1989).

[2] D. Wang, in *Handb. Adv. Magn. Mater.*, edited by Y. Liu, D.J. Sellmyer, and D. Shindo (Springer US, Boston, MA, 2006), pp. 1635–1666.

[3] Y.-J. Zhang, Y.-D. Luo, Y.-H. Lin, and C.-W. Nan, AIP Adv. **5**, 077107 (2015).

[4] J. Nogués, J. Sort, V. Langlais, V. Skumryev, S. Suriñach, J.S. Muñoz, and M.D. Baró, Phys. Rep. **422**, 65 (2005).

[5] W.H. Meiklejohn and C.P. Bean, Phys. Rev. **102**, 1413 (1956).

[6] J.F. Bobo, L. Gabillet, and M. Bibes, J. Phys. Condens. Matter **16**, S471 (2004).

[7] G.A. Prinz, Science **282**, 1660 (1998).

[8] S. Parkin, Xin Jiang, C. Kaiser, A. Panchula, K. Roche, and M. Samant, Proc. IEEE **91**, 661 (2003).

[9] S. Hasan, MSU Grad. Theses (2017).

[10] Y.-H. Lin, B. Zhan, C.-W. Nan, R. Zhao, X. Xu, and M. Kobayashi, J. Appl. Phys. **110**, 043921 (2011).

[11] A. Garg, Growth and Characterization of Epitaxial Oxide Thin Films, Thesis, University of Cambridge, 2001.